CFD and experimental study of convectional heat transfer in free falling particle curtains

Sepideh Afshar and Madoc Sheehan

Citation: AIP Conference Proceedings **1558**, 2005 (2013); doi: 10.1063/1.4825928
View online: http://dx.doi.org/10.1063/1.4825928
View Table of Contents: http://aip.scitation.org/toc/apc/1558/1
Published by the American Institute of Physics

CFD and Experimental Study of Convectional Heat Transfer in Free Falling Particle Curtains

Sepideh Afshar[a] and Madoc Sheehan[b]

[a,b]Department of Chemical Engineering, James Cook University, Townsville, Queensland 4814, Australia

Abstract. The convection heat transfer in particle curtains was studied using a combination of experiments and CFD simulations. The Eulerian-Eulerian approach of CFD has been used to simulate particle curtains. Experiments were conducted with glass beads (290 and 400 μm in mean diameter) flowing through a 20×150mm slot at different mass flow rates (0.06-0.135kg/s). The centreline temperature of particle curtains was determined experimentally using infrared photography. Effects of mass flow rate and particle size on heat transfer have been investigated.

Keywords: CFD, Eulerian-Eulerian, Particle curtains, Infrared thermography

INTRODUCTION

Optimisation of heat transfer in drying industries is very essential, particularly in flighted rotary dryers. Flighted rotary dryers are typical equipments using particle curtains. To design, evaluate and/or simulate flighted rotary dryers it is important to have a good understanding of heat transfer between particle curtains and air. Single particle models are a common approach to approximate both drag and heat transfer. However, it has been observed that the behaviour of a single particle is different to the behaviour of particles in a curtain [1, 2]. Recently Computational Fluid dynamics (CFD) has been successfully applied to model particles in curtains [3-6]. According to isothermal studies of particle curtains by Wardjiman et al. (2008 and 2009), the shape of the curtain has converging and diverging behaviour that is dependent on initial solid volume fraction. Eulerian-Eulerian CFD simulations have been used to model successfully the edge of the curtains [3, 4]. There have been a few simulation techniques used to model heat transfer in particle curtains[5, 7]. Recently a range of techniques using CFD data were applied to identify the average properties of hot particle curtains such as solid volume fraction, mean residence time and edge of the curtain [8].

Hurby et al. (1988) investigated the convective heat transfer of particles in curtain experimentally and numerically. They observed that the drag coefficient on hot particles was higher compared to ambient conditions. Wardjiman and Rhodes (2009) [5] studied the heat transfer of free falling particle curtains experimentally and the single particle model used to compare against model predictions.

Experimental approaches to investigating heat transfer in particle curtains are challenging and there has been lack of significant experimental study despite their prevalence in industrial equipment. These have been dominated by visible imaging, capacitance studies and direct temperature measurement (thermocouples).There are a few examples of the use of applied infrared photography to visualise temperature [9-12]. Recently conductive heat transfer has been investigated using infrared thermal imaging in a fluidised bed [10]. The use of IR images has some advantages compared to standard sensors such as thermocouples, resistance temperature detectors and pyrometers, particularly when dealing with moving objects. Measuring temperature with thermocouples can be inaccurate because they are required to be attached to the object. They are most appropriate for measuring small contact zones and are less suitable for measuring bulk temperature in convective heat transfer applications. IR thermography gives an advantage of measuring the temperature of the surface in two dimensional plane rather than at a particular point such as thermocouples. It allows measuring of the temperature of a solid-state body surface and not that of the surrounding atmosphere [13]. The response time of infrared thermography is typically about 10^{-1} -10^{-2} s [14].With regard to these advantages, it is worthwhile to apply infrared photography to the investigation of heat transfer of particle curtains.

The focus of this work is to compare CFD predictions of centreline temperatures of particle curtains with those obtained experimentally using infrared photography.

11th International Conference of Numerical Analysis and Applied Mathematics 2013
AIP Conf. Proc. 1558, 2005-2008 (2013); doi: 10.1063/1.4825928

EXPERIMENTAL PROCEDURE

The experimental system used in this work is schematically represented in Figure 1 (a, b). The experimental apparatus consisted of the following assemblies: Black background, hopper, spreader box, perforated plates and wire mesh, catch bin, scale indicator, laptop, oven, infrared camera and high speed camera. In Figure 1(a, b) perforated plates and wire mesh, catch bin, scale indicator laptop and high speed camera are out of view.

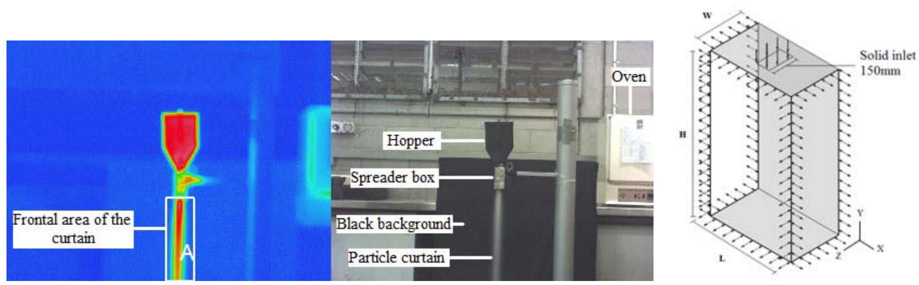

(a) (b) (c)

FIGURE 1. Schematic diagram of experimental set-up showing (a) infrared picture (rectangular area (A)) with approximate image area of 0.092×0.31m (b) standard visible picture (c) Schematic diagram of simulation domain (L=505 mm, H=900 mm and W=300 mm)

The wedge stainless hopper was used to generate mass flow and contained approximately 7kg of hot glass beads. The beads exiting the hopper were fed directly into a spreader box fabricated with wire meshes and perforated plates in order to produce a uniform mass flow across the entire curtain opening. Perforated plates were designed with 40 holes (5mm in diameter). Particles were collected using a catch bin placed on the scale indicator. The scale indicator measured the mass flow rate of particles falling from the hopper. Typical regression coefficient for mass flow rates was 0.98-1. Glass beads were uniformly heated in the oven for three hours. IR images were used to confirm that the mass flow was uniformly distributed, across the opening. High speed camera images were used to measure the initial velocity of particles falling from spreader box. An infrared camera (NEC Avio, H2600 Series) with the resolution of 640×480 pixels was used to visualize the temperature gradient in the particle curtain.

The initial velocity of particles was determined using high speed camera images taken every 0.001 seconds. Images were analysed using ImageJ software and processed by comparison to a single particle model for estimation of initial velocity. The experimental data compared to the range of initial velocities of single particle model. The calculated initial velocity across all runs was 0.23m/s.

CFD MODEL

The CFD Eulerian-Eulerian approach was used to model the falling particle curtains. Hot particles (T_s=400K) fall in a rectangular box filled with air (T_g=300K) with dimensions of 505×900×300mm and a centrally located slot opening at the top of the box with dimensions 20mm by 150mm (Figure 1(c)). Mesh dependency was carried out using average heat loss per unit mass as the convergence criteria. Different mesh size (3mm, 4mm, 5mm, 6mm, 7mm and 8mm) with a mass flow rate of 0.041kg/s were investigated. A mesh size of 5mm with ranging elements of 1,085,400 and 1,120,752 nodes was considered reasonable and was utilised in all simulations. There are four faces bounding the calculation domain: the solid inlet and the three air opening. The remaining walls were governed by the no-slip boundary condition. The glass bead were considered spherical with density of 2500 kg/m^3, average diameter (d_s) of 290µm and 400µm, heat capacity of 830 J/kg K and thermal conductivity of 0.18 W/m K. A full description of the CFD model used in Ansys-CFX is described in Afshar and Sheehan (2012) [15].The model equations include continuity; momentum; energy conservation; drag, turbulence and heat transfer coefficient expressions. The distinctive elements of the CFD simulation equations are shown below. Equation (1) shows the Ranz-Marshall correlation [16] which was used to describe the heat transfer coefficient characterising convection between the air and particle phases. In these simulations Reynolds numbers are less than 50, therefore equation (1) is valid. The particle drag model (C_D) used the commonly used Schiller –Naumann expression shown in equation (2)

[17]. Interphase drag coefficient was used within the Gidaspow model. The turbulence model for continuous phase and dispersed phase were k-ε and Zero-Equation model.

$$Nu = 2 + 0.6Re^{0.5}Pr^{0.3} \qquad 0 \leq Re < 200\,,\ 0 \leq Pr < 250 \tag{1}$$

$$C_D = \begin{cases} \frac{24}{\alpha_g Re}\left[1 + 0.15\left(\alpha_g Re\right)^{0.687}\right] & Re < 1000 \\ 0.44 & Re \geq 1000 \end{cases} \quad \text{where} \quad Re = \frac{\rho_g d_s |\vec{v}_g - \vec{v}_s|}{\mu_g} \tag{2}$$

RESULTS

The surface temperature of particle curtains was recorded using an infrared camera aligned with the narrow end of the slot. Figure 1 (a) shows the frontal area of curtain (rectangular A) visualised using infrared photography. The red regions show the higher temperatures located in the centre of the particle curtain. The green regions represent the cooler areas that are generally at the edge of the curtain, at the interface between particles and air. Dark blue areas are presenting ambient air temperatures. The infrared image (frontal area of the curtain) for ten consequent frames was extracted to an Excel file that includes a matrix of the height and width of the curtain in pixel format, in addition to the temperature of the 2D plane. The centreline temperature was selected to be compared to the CFD results. The centreline temperature profiles for the particle curtain in the experimental results were not always geometrically centred due to subtle horizontal movement of the particle curtain. In order to find the centreline temperature of the particle curtains the maximum temperature in each matrix row was identified using Matlab.

The CFD centreline temperature from the XY plane (at X=0.2525m and Z=0.225m) was compared to the experimental results. Figure 3 (a-d) shows a comparison of centreline temperatures from the experiments and CFD simulations under conditions of varying mass flow rates and varying particle size.

The CFD results are well-matched with experiments when the particle size is small (290µm). At larger particle sizes (400µm) the CFD model is less able to predict the behaviours of particle curtains. The CFD model under-predicts the extent of heat transfer that occurs.

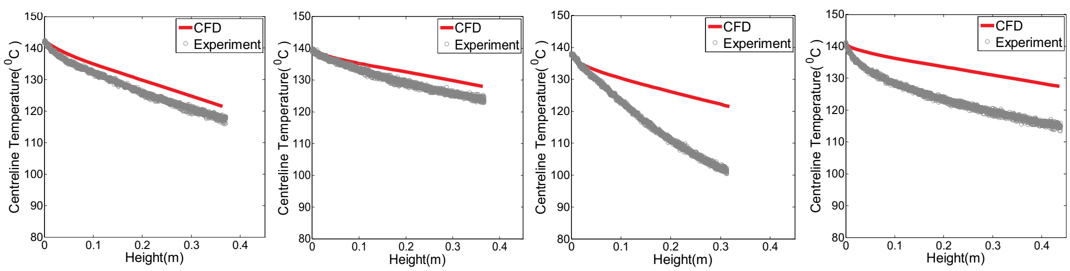

(a) (b) (c) (d)

FIGURE 3. (a) d_s=290µm, m^0 =0.062kg/s and T_g=30.6^{0}C (b) d_s=290µm, m^0 =0.132kg/s, T_g=31.9^{0}C (c) d_s=400µm, m^0 =0.0618kg/s T_g=32^{0}C (d) d_s=400µm, m^0 =0.135kg/s, T_g=32^0

DISCUSSION

The experimental methodology provides a good technique for characterising temperature profiles within particle curtains. It was observed that CFD provides good prediction of the temperature profile for small particle sizes (290µm). However, simulations were not as well-matched with experiments for larger particle sizes (400µm). There are a few potential reasons for this discrepancy. In our CFD simulations the particle size was assumed to be uniform and constant, which was not a true reflection of the experimental conditions. Whilst the size distribution of the small particles (290µm) was narrow, the size distribution of the larger particles was broader. Under the conditions we examined the distances between the larger particles were greater than the distances between the smaller particles. This could lead to the entrainment of more air between the particles and increase the rate of heat loss for the larger particles. However, the volume fraction at the inlet in both situations remained the same. Given the Schiller Naumann drag correlation (16) we used in our simulations is a function of volume fraction, not inter-particle distance, the drag coefficient may not be affected as much as we believe it should be. It is assumed by the authors that the underlying CFD equations, particularly the drag model, are less suited to modelling the behaviour of curtains of large particle sizes. Furthermore, the literature suggests that alternative drag models be considered when modelling hot particles [7, 18]. However, the available models are only suitable for single particle systems.

CONCLUSION

The CFD Eulerian-Eulerian approach was used to predict the centreline temperature profile within hot particle curtains. Infrared photography was used to visualise experimental centreline temperature profiles. The comparison of CFD and experimental data for centreline temperatures showed good agreement for small particles (290µm) at two different mass flow rates. CFD was less able to accurately predict the centreline temperature at larger particle sizes (400µm) irrespective of the mass flow rate. Alternative drag models for larger particle sizes may improve the predictability of Eulerian-Eulerian CFD simulation of particle curtains.

REFERENCES

1. C.G.J. Baker, Air-solids drag in cascading rotary dryers, *Drying Technol.***10**,365 - 393 (1992).
2. K. Ogata, K. Funatsu and Y. Tomita, Experimental investigation of a free falling powder jet and the air entrainment, *Powder Technol.* **115**,90-95 (2001).
3. C. Wardjiman, A. Lee, M.E. Sheehan and M. Rhodes, Shape of a particle curtain falling in stagnant air, *Powder Technol.* **192**,384-388 (2009).
4. C. Wardjiman, A. Lee, M.E. Sheehan and M. Rhodes, Behaviour of a curtain of particles falling through a horizontally-flowing gas stream, *Powder Technol.* **188**,110-118 (2008).
5. C. Wardjiman, M. Rhodes, Heat transfer in a particle curtain falling through a horizontally-flowing gas stream, *Powder Technol*. **191**,247-253 (2009).
6. T. Uchiyama and M. Naruse, Three-dimensinal vortex simulation for particulate jet generated by free falling particles, *Chem. Eng. Sci.* **61**,1913-1921 (2006).
7. J. Hurby,R. Steeper, G. Evans and C. Crowe, An experimental and numerical study of flow and convective heat transfer in freely falling curtain of particles, *J. Fluid Eng.* **110**,172-181(1988).
8. S. Afshar and M.E. Sheehan, CFD methodologies to predict average properties of particle curtains undergoing convection heat transfer, *Appl. Math. Model.* (2013).(submitted).
9. N.K. Akafuah, A.J. Salazar and K. Saito, Infrared thermography-based visualization of droplet transport in liquid sprays, *Infrared Phys. Techn.* **53**,218-226 (2010).
10. J. Yamada, N. Nagahara, I. Satoh and Y. Kurosaki, Direct-Contact heat exchange between fluidizing particles and a heat transfer surface in a fluidized bed: temperature visualization of fluidizing Particles, *Heat transf.Asian res.* **31,**165-181(2002).
11. L. Novak, M. Mori and M. Sekavcnik, Heat transfer study in rotating cascade using IR thermography and CFD analyses, *Heat Mass Transfer* **44**, 559-567 (2008).
12. L.P.C. Neto, M.C.G. Silva and J.J. Costa, On the use of infrared thermography in studies with air curtain devices, *Energ. Buildings* **38**,1194-1199 (2006).
13. H. Budzier and G. Gerlach, *Thermal infrared sensors,Theory,Optimisation and Practice*,Chichester: John Wiley & Sons,Ltd., 2011. pp.7
14. T. Astarita, G. Cardone, G.M. Carlomagno and C. Meola, A survey on infrared thermography for convective heat transfer measurements, *Opt.Laser Technol.* **32**,593-610 (2000).
15. S. Afshar and M.E. Sheehan, Using CFD to simulate heat transfer in particle curtains in: Ninth International Conference on CFD in the Minerals and Process Industries,CSIRO, Melbourne,Australia, (2012).
16. W.E. Ranz and W.R. Marshall, Evaporation from drops, *Chem. Eng. Prog*. **48** 141-146 (1952).
17. L. Schiller and A. Naumann, Über die grundlegenden Berechnun gen bei der Schwekraftaubereitung, *Z. Ver. Dtsch. Ing*. **77**,318-320 (1933).
18. I.P. Basina and I.A. Maksimov, Effect of nonisothermicity on the aerodynamic drag on a spherical particle, *Heat trans. Soviet res.* 2,**69**-75(1970).